

# Characterization of cellulose nanofiber sheets from different refining processes

Kohji Nobuta · Hiroshi Teramura · Hiroaki Ito · Chizuru Hongo · Hideo Kawaguchi · Chiaki Ogino · Akihiko Kondo · Takashi Nishino

Received: 10 March 2015 / Accepted: 19 October 2015 / Published online: 24 October 2015  
© Springer Science+Business Media Dordrecht 2015

**Abstract** Four types of kenaf bast fibers were prepared via a combination of Wise treatments, for delignification, and alkaline treatments, for the removal of hemicellulose. Each type of kenaf bast fiber with different refining processes were nano fibrillated by grinding. Resulting, cellulose nanofiber (CNF) sheet was obtained from CNF by vacuum filtration (Scheme 1). The structures and properties of these CNF sheets then were investigated to determine how the CNF components had affected these properties. All of the CNFs from different refining processes were classified as a cellulose I<sub>β</sub> type by X-ray diffraction. However, the mechanical properties (Young's modulus, tensile strength and toughness) of the CNF sheet with Wise treatment were higher than the properties of the other three CNF sheets. These results strongly suggested that alkaline treatment was unnecessary for the removal of hemicellulose, and that the application of the Wise treatment effectively imparted high mechanical properties to the cellulose microfibrer.

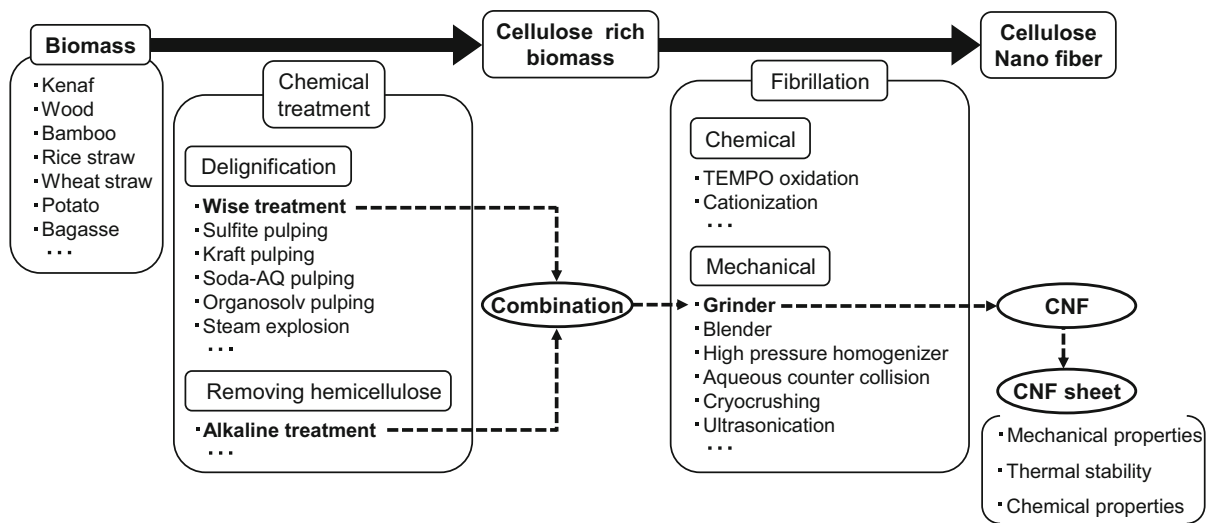
**Keywords** Cellulose nanofiber · Wise treatment · Alkaline treatment · Different refining processes · Mechanical properties

## Introduction

Since the supply of petroleum has become a problem that often is defined as a crisis, an environmental perspective requires the development of new materials, which do not depend on petrochemistry (Nagai and Suzuki 2000; Petersson et al. 2007; Abdul Khalil et al. 2012). New materials with advanced mechanical properties, and environmentally harmonious properties, have been developed from biomass resources such as chitin, chitosan collagen and starch (Nishino et al. 1999; Mohanty et al. 2002; Ifuku et al. 2009; Kaushik et al. 2010). In particular, cellulose is at the center of attention because it is the most abundant biomass resource in nature. Cellulose is also well known to possess high mechanical properties (Nishino et al. 1995), thermal stability (Nishino et al. 2004), and biodegradability, and it is, therefore, expected to be used as a filler for environmentally friendly composites (Nishino and Arimoto 2007; Henriksson et al. 2008; Soykeabkaew et al. 2008, 2009; Fujisawa et al. 2013; Suzuki et al. 2013). In comparisons with glass fiber and synthetics such as carbon fiber, cellulose has the advantage of low density, low cost, and easier handling (Nishino et al. 2004). Several types of biomass have recently been well utilized for the

---

K. Nobuta · H. Teramura · H. Ito · C. Hongo · H. Kawaguchi · C. Ogino · A. Kondo · T. Nishino (✉)  
Department of Chemical Science and Engineering,  
Graduate School of Engineering, Kobe University,  
Rokko, Nada, Kobe 657-8501, Japan  
e-mail: tnishino@kobe-u.ac.jp



**Scheme 1** Schematic roots for getting cellulose nanofiber from biomass with various treatments and fibrillation methods

development of new materials: wood, bamboo, rice straw, wheat straw, potato, bagasse, hemp etc. (Cao et al. 2006; Abe and Yano 2009; Kaushik et al. 2010; Puangsin et al. 2013; Saito et al. 2013). Among them, kenaf (*Hibiscus cannabinus*, L. family Malvaceae) has gained popularity for use as a biomass material, because it is an herbaceous annual plant that can be grown under a wide range of weather conditions. For example, kenaf grows to more than 3 m within 3 months even under moderate ambient conditions (Nishino et al. 2003). In addition, kenaf fiber also exhibits several advantageous properties: low density, non-abrasiveness during processing, high specific mechanical properties, and biodegradability. Thus, application of kenaf fiber has been emerged, recently (Charles et al. 2002; Nishino et al. 2003).

Recently, by subjecting of these good properties of biomass, nano-sized plant cellulose fibrils, namely cellulose nanofibers (CNFs), has been well investigated (Nogi et al. 2009; Okahisa et al. 2009; Liu et al. 2011; Yousefi et al. 2011; Yang et al. 2013). Nanofibers possess a high specific surface area, thus, common sense dictates that the entanglements and interactions of each fibril would produce high frequencies. Based on these nanofiber properties, CNFs also exhibit high mechanical properties (Yousefi et al. 2011; Saito et al. 2013), transparency (Fukuzumi et al. 2009; Nogi et al. 2009), and gas barrier properties (Fukuzumi et al.

2009; Liu et al. 2011; Yang et al. 2012). Thus, CNFs are expected to be applicable as structural materials for automobiles (Iwatake et al. 2008), for the reinforcement of composite and organic glasses (Nogi and Yano 2008), as packaging for food and medical supplies (Fukuzumi et al. 2009; Liu et al. 2011), gas separation membranes (Fukuzumi et al. 2013), and as flexible electronic substrates (Okahisa et al. 2009). Moreover, since it also showed high viscosity in water, nanofibers have also been applied as a thickener for food (Qua et al. 2009).

CNFs are commonly prepared via fibrillation (chemical treatment and mechanical fibrillation) after removal of the lignin and hemicellulose from the original biomass via chemical treatment (Scheme 1) (Nogi et al. 2009; Okahisa et al. 2009), which has traditionally consisted of two processes: delignification and the removal of hemicellulose. Delignification is usually performed via processes that include sulfite pulping (Gierer 1985), kraft pulping (sulfate pulping process) (Gierer 1985), soda pulping (Gierer 1985), organosolv pulping (Johansson et al. 1987), steam explosion (Li et al. 2007), and treatment with sodium chlorite ( $\text{NaClO}_2$ ) (namely, the Wise treatment) (Wise et al. 1946; Yano et al. 2001). Alkaline treatment efficiently removes hemicellulose (Wise and Evelyn 1947) when plant biomass is immersed into either a sodium hydroxide or a potassium hydroxide solution with heating.

Fibrillation of cellulose rich biomass into nanofibers can be roughly divided into two strategies: chemical and mechanical fibrillation. In the case of chemical fibrillation, two methods have been thoroughly investigated: 2,2,6,6-tetramethylpiperidine-1-oxyl radical (TEMPO) oxidation (Saito et al. 2006, 2007) and cationization (Pei et al. 2013). For mechanical fibrillation, several methods are available: grinding (Taniguchi and Okamura 1998), blender (Uetani and Yano 2011), high pressure homogenizer (Henriksson et al. 2008), aqueous counter collision (Kose and Kondo 2011), cryocrushing (Dufresne et al. 1997), and ultrasonication (Zhao et al. 2007). In brief, during the fibrillation, the plant fibers are difficult to separate due to the presence of lignin and hemicellulose in the inter fibril region of biomass. Therefore, the residual components of lignin and hemicellulose in CNF drastically affect the change of CNF properties. There are several reports concerning the relationship between chemical treatment processing and the resultant properties of CNF (Iwamoto et al. 2008; Jonoobi et al. 2009; Karimi et al. 2014). Mainly, these reports focused on the investigation of relationship between chemical treatment processing and CNF thermal properties. In addition, there are no reports concerning the relationship between chemical treatment processing and the mechanical properties of CNF.

In this study, Wise treatment and alkaline treatment were used for delignification and for removal of hemicellulose, respectively, during the evaluation of kenaf bast fiber. In detail, kenaf bast fibers were prepared using a combination of the above two methods, then grinding was used to form CNFs. Four CNF sheets then were prepared by vacuum filtration, and the structures and properties of these CNF sheets were investigated (Scheme 1).

## Experimental

### Materials

Kenaf bast fiber (length:2 [mm]) was kindly supplied by the Toyota Boshoku Corporation (Aichi, Japan). Impurities in the kenaf bast fiber were removed using a 1 mm sieve. The other chemicals used (sodium chlorite, acetic acid, potassium hydrate, zinc chloride, acetic anhydride, and ethanol) in this study were purchased from Nacalai tesque, Inc. (Kyoto, Japan).

### Purification process of kenaf bast fibers

In this study, two kinds of chemical treatment methods [Wise treatment (NaClO<sub>2</sub> treatment) (Yano et al. 2001), and alkaline treatment (Wise and Evelyn 1947) as mentioned below] were applied for biomass treatment, as shown in Fig. 1. Using combinations of the two treatments, four kinds of pretreated biomass were prepared for evaluation. After degreasing the kenaf bast fiber, the following four samples were individually prepared: a sample with no chemical treatment except for degreasing [referred to as (O)]; Wise treatment (W); alkaline treatment (A); and, a sample that applied an alkaline treatment after a Wise treatment (R). The details of the protocols used for each of these treatments are described below.

### Degreasing

Kenaf bast fibers, 20 g, were degreased via Soxhlet extraction using a 1:2 (v/v) mixture of ethanol/toluene for 20 h at 78 °C (78 °C: azeotropic temperature). Kenaf-bast fibers then were washed 3 times with ethanol, then dried *in vacuo* at 50 °C for 12 h.

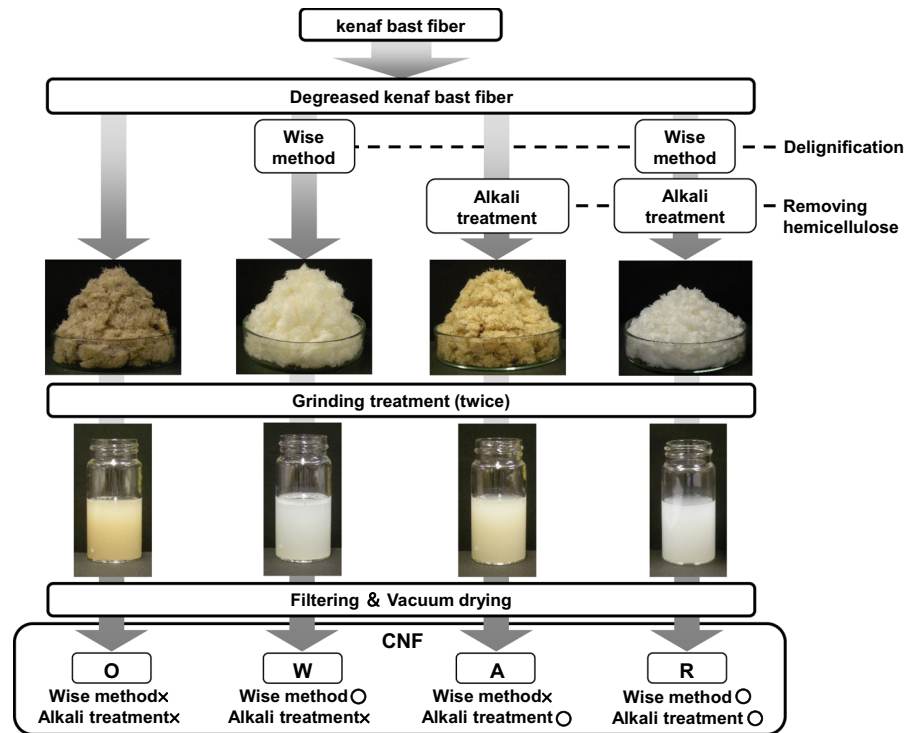
### Wise treatment

A residual fraction of degreased biomass was suspended in 1 L of distilled water, and the following treatment was applied. In order to remove the lignin from a sample, sodium chlorite, 6.7 g, was directly added to the biomass suspension described above with gentle mixing, and acetic acid, 1.2 ml, was subsequently added. The biomass suspension mixture then was incubated at 80 °C for 1 h. The addition of sodium chlorite, 6.7 g, and acetic acid, 1.2 ml, was repeated 5 times in 1 h intervals. Finally, the mixture was filtered using filter paper No. 1 (Advantech Toyo Kaisha, Ltd., Tokyo, Japan), and the solid fraction was rinsed 5 times with distilled water. The rinsed sample was maintained in a semi-wet state at 4 °C until use.

### Alkaline treatment

In order to eliminate the hemicellulose from the biomass, the degreased biomass was allowed to dry (or semi-wet biomass after Wise treatment), then it was soaked with 4 wt% potassium hydrate solution, 0.5 L, at 80 °C for 2 h. The reaction mixture was filtered

**Fig. 1** Preparation of kenaf nanofiber sheets with various treatments



with filter paper no. 1, and the filtrate sample was rinsed 3 times with distilled water. This operation was repeated twice. Finally, the mixture was filtered using filter paper No. 1, and the solid fraction was rinsed 5 times with distilled water. The rinsed sample was maintained in a semi-wet state at 4 °C until use.

#### Preparation of the CNF sheets

Finally, each kenaf bast fiber sample (O, W, A, and R) was suspended with distilled water, 1 L, and passed twice through a grinder (MKCA6-2, Masuko Sangyo Co., LTD., Saitama, Japan) at 1500 rpm. The resultant CNF dispersions were adjusted to a concentration of 0.5 wt% via a dry gravimetric method. A CNF dispersion, 130 g, 0.5 wt%, was defoamed using a MAZERUSTAR (Kurabo Industries Ltd., Osaka, Japan) with mixing, and was subjected to filtration as follows. First, a CNF sheet was obtained by vacuum filtration using a polytetrafluoroethylene membrane filter (0.1 μm pore size). Then, each CNF sheet in a semi-wet state was dried *in vacuo* at 50 °C for 12 h, and tested for following characterization of CNF sheet, as described below. The CNF sheets were

similar in size with an average thickness of between 60 and 70 μm.

#### Field emission scanning electron microscopy (FE-SEM)

Each CNF was observed using a field-emission scanning electron microscope, FE-SEM (JSM-7500, JEOL, Tokyo, Japan) at an accelerating voltage of 5 kV. Pt/Pd was deposited onto the surfaces prior to the observation, according to instruction protocols.

#### Fourier transform infrared spectrophotometer (FT-IR)

Fourier transform infrared spectroscopy (FTIR) measurements were performed with an FT-IR spectrophotometer (Spectrum GX, PerkinElmer Co., Ltd., Massachusetts, USA) with 4 cm<sup>-1</sup> resolution, and the spectra measurement was repeated 10 times. The spectra were recorded in the transmission mode using the KBr method at wavenumbers that ranged from 400 to 4000 cm<sup>-1</sup>.

## X-ray diffraction

The structures of the CNF sheets were investigated using X-ray diffraction with symmetric reflection geometry. X-ray diffraction profiles were obtained using  $\text{CuK}\alpha$  radiation ( $\lambda = 1.5418 \text{ \AA}$ ) from a RINT-2000 (RIGAKU Co., Tokyo, Japan) under the following conditions: 40 kV, 20 mA, scan speed  $0.5^\circ/\text{min}$ , sampling step angle  $0.02^\circ$ , and scan range  $2\theta = 5^\circ\text{--}40^\circ$ .

Crystallinity ( $CrI$ ) was calculated using the *Segal's* method with Eq. (1) (Segal et al. 1959).

$$CrI = \frac{(I_c - I_a)}{I_c} \quad (1)$$

In this equation,  $I_c$  means the maximum intensity at  $2\theta$  was between  $22^\circ$  and  $23^\circ$  for cellulose I, and  $I_a$  refers to the minimum intensity at  $2\theta$  for cellulose I. Crystallite size  $D$  was calculated using *Scherrer's* Eq. (2) (Nishino et al. 2004; Abbott and Bismarck 2010).

$$D = \frac{\lambda}{\beta \cos \theta} \quad (2)$$

In the calculation of  $D$ ,  $\lambda$ , and  $\beta$ ,  $\theta$  were indicated at  $1.5418 \text{ \AA}$ , for a corrected integral width, and Bragg angle for a 200 reflection using this equation, respectively.

## Tensile test

The stress–strain curves of each CNF sheet were measured using a tensile tester (Autograph AGS-1kND, Shimadzu, Kyoto, Japan) at room temperature. A rectangular-shaped specimen ( $5 \text{ mm} \times 40 \text{ mm}$ ) of a CNF sheet was formed using a cutter, and the specimen was completely dried *in vacuo* at  $40^\circ \text{C}$  more than 12 h before use. The initial length of the specimen was 20 mm, and the extension rate was 1 mm/min. A cross-sectional area was evaluated using the density, the weight, and the length of the samples. Density was measured using the floatation method (benzene/carbon tetrachloride system) at  $30^\circ \text{C}$ . The average values and standard deviation of Young's modulus, tensile strength and strain at break were evaluated using five independent specimens, and each data was averages of five independent experiments  $\pm$  standard deviation

(Table 1). The toughness was calculated by unit weight (Boncel et al. 2011; Morimune et al. 2011).

## Dynamic mechanical analysis (DMA)

The dynamic storage modulus,  $E'$ , was measured using a dynamic mechanical analyzer (DVA-220S, ITK, Ltd., Osaka, Japan) at temperatures ranged from  $-150$  to  $200^\circ \text{C}$ . The sample was cut into  $30 \text{ mm} \times 5 \text{ mm}$  pieces for measurement. The heating rate was  $6^\circ \text{C}/\text{min}$ , the initial length was 20 mm, and the tensile frequency was 10 Hz. A tensile deformation of 0.15 % was applied to each specimen.

## Thermal expansion behavior

Thermomechanical analysis was performed using a thermomechanical analyzer, (Thermo plus EVOII TMA8310, Rigaku Co., Tokyo, Japan) with temperatures ranged from  $30$  to  $110^\circ \text{C}$  at a heating rate of  $10^\circ \text{C}/\text{min}$ . The sample was cut into  $25 \text{ mm} \times 2 \text{ mm}$  pieces, and the specimen was dried at  $40^\circ \text{C}$  for 12 h prior to measurement. The specimen with an original length of 20 mm was subjected to a uniaxial stress of 1 MPa, and its thermal expansion coefficient  $\alpha$  was defined between 100 and  $120^\circ \text{C}$ .

## Sugar analysis

Equal amounts ( $1.5 \mu\text{L}$ ) of each sample and 0.1 % w/w ribitol were added to tubes and dried using a vacuum concentrator (7810010; Labconco, Kansas City, MO). The resultant residue was dissolved in  $100 \mu\text{L}$  of a mixture of 20 mg/mL of methoxyamine hydrochloride in pyridine, which was then incubated at  $30^\circ \text{C}$  for 90 min. After incubation,  $50 \mu\text{L}$  of *N*-methyl-*N*-trimethylsilyltrifluoroacetamide (MSTFA) was added to the sample solution with incubation at  $37^\circ \text{C}$  for 30 min. Aliquots of sample solutions ( $10 \mu\text{L}$ ) were subjected to gas chromatography-mass spectrometry (GCMS-2010 Plus; Shimadzu, Kyoto, Japan) under the following conditions: column, Agilent CP-Sil 8CB-MS ( $30 \text{ m} \times 0.25 \text{ mm}$ ); carrier gas, helium; injection temperature,  $230^\circ \text{C}$ ; oven temperature,  $80^\circ \text{C}$  at  $t = 0\text{--}2 \text{ min}$ , then to  $330^\circ \text{C}$  at  $15^\circ \text{C min}^{-1}$  (Matsuda et al. 2011).

**Table 1** Density, Young's modulus ( $E$ ), tensile strength ( $\sigma_{max}$ ), strain at break ( $\varepsilon_{max}$ ), and toughness ( $K$ ) of CNF sheets with O, W, A, and R treatments

Sample	Density (g/cm <sup>3</sup> )	Young's modulus $E$ (GPa)	Tensile strength $\sigma_{max}$ (MPa)	Strain at break $\varepsilon_{max}$ (%)	Toughness $K$ (J/g)
O	1.47	7.9 ± 0.3	123 ± 11	2.2 ± 0.5	1.1
W	1.49	10.3 ± 0.3	209 ± 15	4.8 ± 0.7	5.5
A	1.50	8.4 ± 0.7	136 ± 17	3.7 ± 1.1	1.8
R	1.53	8.6 ± 0.5	160 ± 9	4.5 ± 0.8	3.6

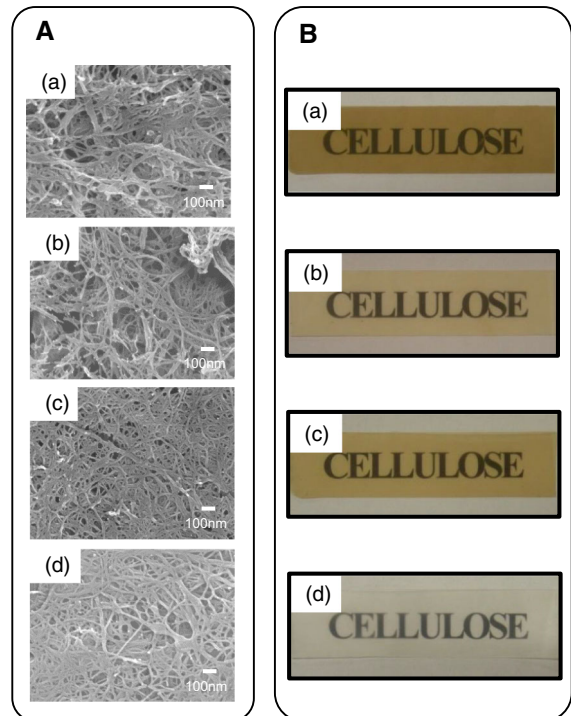
### Compositional analysis of biomass

The composition of raw materials was determined using a standard analysis procedure for biomass composition, which was a modification of the National Renewable Energy Laboratory (NREL) analytical method. Following two-step acid hydrolysis, the polysaccharide composition was determined based on the monomer content. In the first step, 3 ml of 72 % w/w sulfuric acid was added to 300 mg of dried raw biomass, followed by incubation at 30 °C for 2 h. In the second step, the reaction mixture was diluted to 4 % w/w with deionized water and was autoclaved at 121 °C for 1 h. The hydrolysis solution was neutralized to pH 5.0 with the addition of powdered calcium hydroxide. The sugar content of the liquid hydrolysate was determined by GCMS under the conditions described above.

## Results and discussion

### Characterization of CNF

Conventional wisdom held that CNF could not be obtained without treatment of the plant fiber. Therefore, various bast fibers that had been treated with different refining processes were subjected to the grinding treatment (Fig. 1). To distinguish which nanofibers had been prepared from the various bast fibers, the FE-SEM images of four types of CNF sheets were observed (Fig. 2A). The fiber diameters of O, W, A, and R were 20, 18, 18, and 17 nm, respectively. The fiber diameters in each of the CNF sheets were less than 100 nm, and these results agreed well with the definition of a nanofiber. These results strongly indicated that these CNF sheets, which were prepared from kenaf bast fibers using four different types of

**Fig. 2** A SEM images and B Optical transparency of CNF sheets with (a) O, (b) W, (c) A, and (d) R treatments

refining processes, could form a fibrillated fiber state with a nanostructure. These results did not agree with one previous article (Chang et al. 2012). These differences will be caused by the number of grinding passes. The CNF sheets were prepared using the same protocol and the same concentrations of CNF dispersion. The thicknesses of CNF sheets O, W, A and R were 69, 65, 63, and 60 μm, respectively. Every CNF sheet showed good transparency (Fig. 2B), and these results agreed well with previous articles (Nogi et al. 2009; Yousefi et al. 2011), which strongly indicated that kenaf bast fiber will form CNF even with different refining processes.

## Mechanical properties

In order to measure the mechanical properties, a tensile test was performed for each CNF sheet. All CNF sheets showed a stress ( $\sigma$ )–strain ( $\varepsilon$ ) curve for brittle materials without a clear yielding point (Fig. 3). The value of Young's modulus ( $E$ ), tensile strength ( $\sigma_{max}$ ), strain at break ( $\varepsilon_{max}$ ), and toughness ( $K$ ) increased in the following order for the CNF sheets: O, A, R, and W (Table 1). In the preparation of a CNF with colorless and transparent characteristics using chemical treatments such as TEMPO-mediated oxidation or mechanical treatments (Taniguchi and Okamura 1998; Abe and Yano 2009; Nogi et al. 2009; Okahisa et al. 2009, 2011; Yousefi et al. 2011), a completely refined plant fiber was usually used because the lignin and hemicellulose fraction that remained in the interfiber were believed to inhibit its fibrillation, and to induce low mechanical properties. In study, however, by combining degreasing and Wise treatment, CNF sheet W showed the highest mechanical properties. The values for strain at the break of CNF sheets W and R were larger than those of CNF sheets O and A. When the hydrophobic lignin that had presented on the hydrophilic cellulose surface was removed and/or denatured by Wise treatment, the interfibril hydrogen bond was enhanced (Iwatake et al. 2008). Thus, each fibril was incapable of slipping, which resulted in increases in the mechanical properties. The mechanical properties of CNF sheet R were lower than those of CNF sheet W, because cellulose

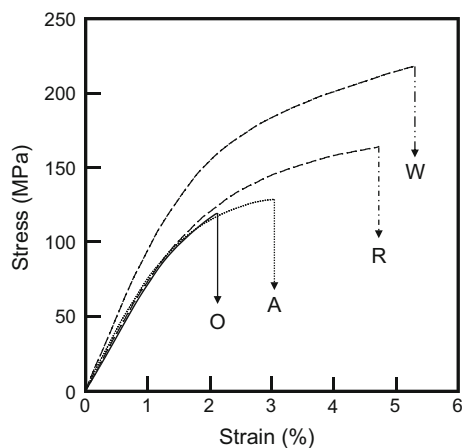


**Fig. 3** Stress ( $\sigma$ )–strain ( $\varepsilon$ ) curves of CNF sheets with O, W, A, and R treatments

that is exposed via alkaline treatment shows damages to the fiber (Knill and Kennedy 2003). These tensile results show that in order to simultaneously attain a high Young's modulus, high tensile strength, high strain at the break, and a high toughness, it was necessary to use with Wise treatment. The Young's modulus obtained from tensile test was performed only at room temperature. Actually, when applying these materials, the effect of temperature on the elastic modulus validation must be evaluated. The temperature dependence of dynamic storage modulus,  $E'$ , of all the CNF sheets was measured using dynamic viscoelastic equipment (Fig. 4A). With decreasing temperature, the  $E'$  of each of the CNF sheets increased. This tendency was related to the molecular motion restriction that is caused by temperature decreases.

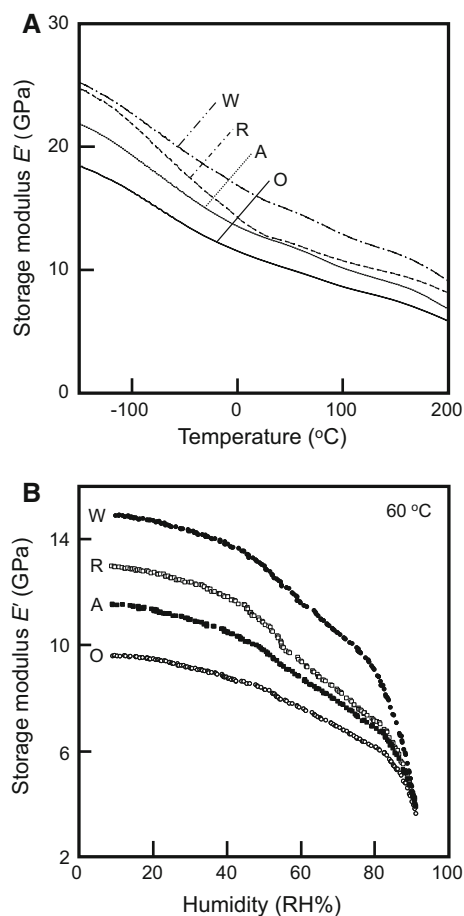


**Fig. 4** **A** Temperature dependence and **B** humidity dependence at 60 °C of the dynamic storage modulus ( $E'$ ) of CNF sheets with O, W, A, and R treatments

The  $E'$  of CNF sheet O was lower than that of CNF sheet R, which agreed well with the results of tensile test (Fig. 3). The  $E'$  value of CNF sheet W showed a 25.2 GPa at  $-150$  °C and a 9.07 GPa at 200 °C. The  $E'$  of CNF sheet W was the highest at room temperature and also for temperatures ranging from  $-150$  to 200 °C. These results indicated that in order to maintain an  $E'$  value even at high temperatures, it is necessary to use Wise treatment. In addition, in the case of humidity dependence of the  $E'$  value as well as temperature dependence, that of CNF sheet O was the lowest and that of CNF sheet W was the highest (Fig. 4B). Furthermore, the decreasing trends of  $E'$  for CNF sheets W, A and O resembled one another at 50 RH%, or more. For CNF sheet R, however, the  $E'$  value decreased significantly compared with those of the others. This is considered to be caused by hydrophobic lignin presented between the fibers of CNF sheet W, A and O. In other words, the hydroxyl group in the cellulose fraction of CNF sheet R appeared as a result of the Wise and alkaline treatments. Therefore, the cellulose fraction of CNF sheet R would have absorbed more easily (Ansari et al. 2014), which would have significantly decreased the  $E'$  value.

#### Thermal stability of CNF sheets

For application of CNF sheet to composite filler, it was also required the assessment of material thermal properties, in particular, the expansion ability. The linear thermal expansion behavior of each CNF sheet was measured (Fig. 5). Every CNF sheet exhibited thermal expansion phenomena as temperature increased, and the linear thermal expansion coefficient of CNF sheet O,  $\alpha_O$ , was  $1.96 \times 10^{-5} \text{ K}^{-1}$ . The  $\alpha_R$  was  $1.67 \times 10^{-5} \text{ K}^{-1}$ , which agreed well with the results of a previous report (Iwamoto et al. 2007). The  $\alpha_R$  was smaller than the  $\alpha_O$ , because lignin in the interfibril region inhibited the creation of a network of hydrogen bonds between the cellulosic fractions. In addition, the  $\alpha_W$  was  $1.44 \times 10^{-5} \text{ K}^{-1}$ , which was the lowest. The results of the tensile test showed the same tendency (Fig. 3); the appearance of a hydrogen bond was induced by the enhancement of network creation between the interfibrils. The  $\alpha$  value decreased in the following order for the CNF sheets: O, A, R, and W. The order of the  $\alpha$  values corresponded with the order of the mechanical properties based on the tensile test.

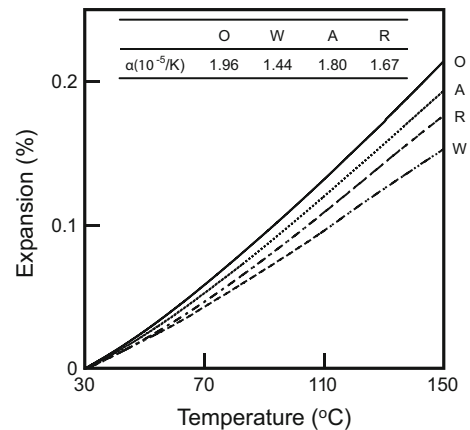


**Fig. 5** Thermal expansion behavior of CNF sheets with O, W, A, and R treatments under 1 MPa

These results showed that a CNF sheet with a higher elastic modulus and a higher tensile strength reflected lower thermal expansion properties for the CNF.

#### Chemical properties of CNF sheets

To analyze the effects of the Wise and alkaline treatments on the chemical changes of the fibers, an FT-IR spectra analysis of each CNF sheet was performed (Fig. 6). The appearance of a glucopyranose ( $1050 \text{ cm}^{-1}$ ) ring in each CNF, showed that the Wise and alkaline treatments had no effect on the polysaccharide structures of either the cellulose or the hemicellulose (Abe et al. 2007; Abe and Yano 2009).

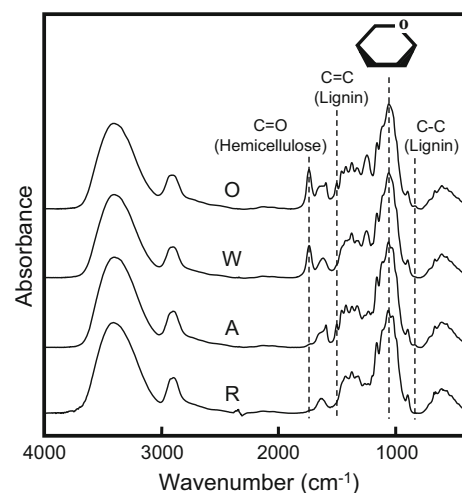


**Fig. 6** FT-IR spectra of CNF sheets with O, W, A, and R treatments



In addition, the adsorptions of the C=C ( $1510\text{ cm}^{-1}$ ) band, the C–C ( $860\text{ cm}^{-1}$ ) band, and the C=O stretching band ( $1750\text{ cm}^{-1}$ ) appeared in CNF sheet O (Sun et al. 2000; Chen et al. 2011; Jonoobi et al. 2011; Chang et al. 2012). On the other hand, the C=C ( $1510\text{ cm}^{-1}$ ) band disappeared from the FT-IR spectrum of CNF sheet W, the C=O stretching band ( $1750\text{ cm}^{-1}$ ) disappeared in CNF sheet A, and both bands disappeared in CNF sheet R. It was considered that phenol ring of lignin would be opened by Wise treatment, and a carbonyl group of the hemicellulose side chain was cleaved by alkaline treatment (Chen et al. 2011; Jonoobi et al. 2011; Kargarzadeh et al. 2012).

#### X-ray diffraction (XRD) of the CNF sheets

We wondered whether the difference in mechanical properties and the crystalline features of cellulose would be related. Therefore, we performed X-ray diffraction measurements (Fig. 7). All CNF sheets belonged to cellulose  $I_{\beta}$ , which is typical for natural plant cellulose. The Wise and alkaline treatments did not affect the crystallites of the cellulose (Chen et al. 2011; Jonoobi et al. 2011; Kargarzadeh et al. 2012). The crystallite size for the (200) plane and the crystallinity of each of the CNF sheets was calculated from the X-ray diffraction peak profiles (Table 2). It was revealed that the crystallite size and crystallinity changed depending on the refinement process. In

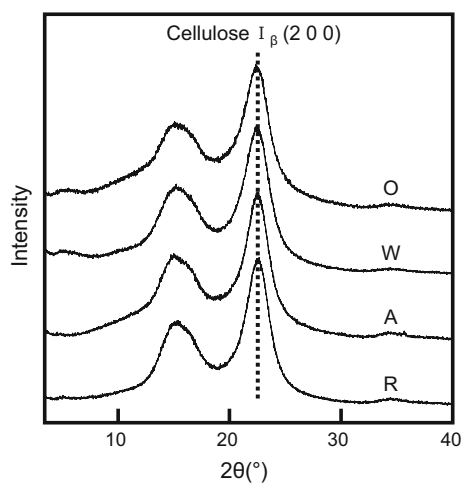


**Fig. 7** X-ray diffraction profiles of CNF sheets with O, W, A, and R treatments

addition, the crystallinity of CNF sheets W and R, which included fractions of hemicellulose and lignin, were higher than that of CNF sheet O. It was considered that amorphous regions in cellulose could be depolymerized by Wise method (Kantouch et al. 1970). By comparing the crystallinity value of 4 sample between Segal's method and area method (Nishino and Arimoto 2007) at X-ray diffraction, the tendency was well agreed. From this result, it was assumed that the high mechanical properties and thermal dimensional stability of CNF sheets W and R were based on high crystallinity. On the other hand, the crystallite size and the mechanical properties were hardly connected.

#### Component analysis of the pretreated kenaf-bast fibers (O, W, A, and R)

The component analysis of the bast fibers before CNF formation was performed to reveal the contents of cellulose, hemicellulose and lignin (Table 3). In the case of O, glucose and xylose were 65.7 and 15.5 wt%, respectively. Assuming hemicellulose consisted of equal parts glucose and xylose, the contents of cellulose, hemicellulose, and others (lignin and ash) were 50.1, 31.0, and 18.8 wt%, respectively. These analytical results agreed well with the data reported for kenaf (Khristova et al. 1998; Kargarzadeh et al. 2012). After the Wise and alkaline treatments (R), the hemicellulose and lignin were drastically decreased to 18.8 and 5.5 wt%, respectively. However, when either Wise or alkaline treatments were used (W or A), the lignin content was similar to that of O, and the content of hemicellulose was not drastically decreased. After a Wise treatment (W), a decrease of hydrophobicity of lignin was observed by FT-IR (Fig. 6), but the removal of lignin could not be confirmed by component analysis. This was because the lignin itself was tightly connected to the hemicellulose via a carbonyl

**Table 2** Crystallinity and crystallite size of CNF sheets with O, W, A, and R treatments

Sample	Crystallinity (%)	Crystallite size (Å)
O	69.4	36.6
W	76.0	37.4
A	73.2	41.2
R	76.8	39.2

**Table 3** Ingredient composition of CNF sheets with O, W, A, and R treatments

Sample	Glucose (wt%)	Xylose (wt%)	Lignin + ash (wt%)
O	65.7	15.5	18.8
W	67.4	17.0	15.6
A	69.6	13.0	17.4
R	85.1	9.4	5.5

group (Grabber 2005; Scheller and Ulvskov 2010; Chen et al. 2011; Jonoobi et al. 2011; Kargarzadeh et al. 2012). After alkaline treatment (A), the carbonyl group connecting the hemicellulose and lignin was cleaved, and the resultant free hemicellulose was released from the fiber (Grabber 2005; Scheller and Ulvskov 2010; Chen et al. 2011; Jonoobi et al. 2011; Kargarzadeh et al. 2012). However, fiber (A) remained hydrophobic since lignin remained within the fiber, and the hemicellulose fraction connected with lignin also remained. After both Wise and alkaline treatments (R), the synergistic effect of the two treatments resulted in both carbonyl group cleavage and lignin hydrophobicity, which resulted in the dissolving of lignin and hemicellulose in water and in an enhancement of the cellulose content in the fiber of R. These results were reflected in the color and density of the CNF sheets (Fig. 2B). Therefore, in order to increase the mechanical properties, the hydrophilic treatment of lignin was more important than the removal of lignin. In addition, it was assumed that the alkaline treatment would cause serious damage to the fibers, which would not enhance the mechanical properties inherent in cellulose for the formation of CNF.

## Conclusions

Conventional wisdom held that CNF should be prepared from cellulose fiber containing no extra for high mechanical properties. However, this study showed that CNF subjected to only Wise treatment possessed a higher mechanical properties than that of CNF subjected to both Wise and alkaline treatments. CNF sheet W maintained a high storage modulus through the entire temperature range (−150 to 200 °C) and through high humidity. Moreover, the  $\alpha$  value of CNF sheet W was lower than that of CNF sheet R. X-ray diffraction indicated that CNF sheet W possessed crystallinity that was as high as that of CNF sheet R. In addition, in CNF sheet W, the cellulose fiber was not damaged by

alkaline treatment, which is considered to be indicative of high mechanical properties. Without the removal of either lignin or hemicellulose, the hydrophobicity of the lignin was changed to hydrophilic, which enabled the preparation of CNF with high mechanical properties. CNF sheet W is expected to be useful in applications requiring durability, heat resistance, humidity resistance, and thermal dimensional stability—as paper for cooking, ventilation ducts, structural members of cars, and as fillers for tires and insulation boards.

**Acknowledgments** We gratefully acknowledge the technical assistance from Tomoko Ohshima. This work was partly supported by Grants-in-Aid from the NC-CARP project and the Ministry of Education, Culture, Sports, Science and Technology, Japan to Kobe University, and Special Coordination Funds for Promoting Science and Technology, Creation of Innovation Centers for Advanced Interdisciplinary Research Areas (Innovative Bioproduction, Kobe) from the Ministry of Education, Culture, Sports, Science and Technology, Japan.

## References

- Abbott A, Bismarck A (2010) Self-reinforced cellulose nanocomposites. *Cellulose* 17:779–791. doi:10.1007/s10570-010-9427-5
- Abdul Khalil HPS, Bhat AH, Ireana Yusra AF (2012) Green composites from sustainable cellulose nanofibrils: a review. *Carbohydr Polym* 87:963–979. doi:10.1016/j.carbpol.2011.08.078
- Abe K, Yano H (2009) Comparison of the characteristics of cellulose microfibril aggregates of wood, rice straw and potato tuber. *Cellulose* 16:1017–1023. doi:10.1007/s10570-009-9334-9
- Abe K, Iwamoto S, Yano H (2007) Obtaining cellulose nanofibers with a uniform width of 15 nm from wood. *Biomacromolecules* 8:3276–3278. doi:10.1021/bm700624p
- Ansari F, Galland S, Johansson M et al (2014) Cellulose nanofiber network for moisture stable, strong and ductile bio-composites and increased epoxy curing rate. *Compos Part A Appl Sci Manuf* 63:35–44. doi:10.1016/j.compositesa.2014.03.017
- Boncel S, Sundaram RM, Windle AH, Koziol KKK (2011) Enhancement of the mechanical properties of directly spun CNT fibers by chemical treatment. *ACS Nano* 5:9339–9344. doi:10.1021/nn202685x

- Cao Y, Shibata S, Fukumoto I (2006) Mechanical properties of biodegradable composites reinforced with bagasse fibre before and after alkali treatments. *Compos Part A Appl Sci Manuf* 37:423–429. doi:[10.1016/j.compositesa.2005.05.045](https://doi.org/10.1016/j.compositesa.2005.05.045)
- Chang F, Lee SH, Toba K et al (2012) Bamboo nanofiber preparation by HCW and grinding treatment and its application for nanocomposite. *Wood Sci Technol* 46:393–403. doi:[10.1007/s00226-011-0416-0](https://doi.org/10.1007/s00226-011-0416-0)
- Charles LW, Bledsoe VK, Bledsoe RE (2002) Kenaf harvesting and processing. *Trends New Crop New Uses* 9:340–347
- Chen W, Yu H, Liu Y et al (2011) Isolation and characterization of cellulose nanofibers from four plant cellulose fibers using a chemical-ultrasonic process. *Cellulose* 18:433–442. doi:[10.1007/s10570-011-9497-z](https://doi.org/10.1007/s10570-011-9497-z)
- Dufresne A, Cavaille J, Vignon MR (1997) Mechanical behavior of sheets prepared from sugar beet cellulose microfibrils. *Sugar Beet Cellul Microfibrils* 64:1185–1194. doi:[10.1002/\(sici\)1097-4628\(19970509\)64:6<1185:aid-app19>3.0.co;2-v](https://doi.org/10.1002/(sici)1097-4628(19970509)64:6<1185:aid-app19>3.0.co;2-v)
- Fujisawa S, Saito T, Kimura S et al (2013) Surface engineering of ultrafine cellulose nanofibrils toward polymer nanocomposite materials. *Biomacromolecules* 14:1541–1546. doi:[10.1021/bm400178m](https://doi.org/10.1021/bm400178m)
- Fukuzumi H, Saito T, Iwata T et al (2009) Transparent and high gas barrier films of cellulose nanofibers prepared by TEMPO-mediated oxidation. *Biomacromolecules* 10:162–165. doi:[10.1021/bm801065u](https://doi.org/10.1021/bm801065u)
- Fukuzumi H, Fujisawa S, Saito T, Isogai A (2013) Selective permeation of hydrogen gas using cellulose nanofibril film. *Biomacromolecules* 14:1705–1709. doi:[10.1021/bm400377e](https://doi.org/10.1021/bm400377e)
- Gierer J (1985) Chemistry of delignification—part 1: general concept and reactions during pulping. *Wood Sci Technol* 19:289–312. doi:[10.1007/BF00350807](https://doi.org/10.1007/BF00350807)
- Grabber JH (2005) How do lignin composition, structure, and cross-linking affect degradability? A review of cell wall model studies. *Crop Sci* 45:820–831
- Henriksson M, Berglund LA, Isaksson P et al (2008) Cellulose nanopaper structures of high toughness. *Biomacromolecules* 9:1579–1585. doi:[10.1021/bm800038n](https://doi.org/10.1021/bm800038n)
- Ifuku S, Nogi M, Abe K et al (2009) Preparation of chitin nanofibers with a uniform width as  $\alpha$ -chitin from crab shells. *Biomacromolecules* 10:1584–1588. doi:[10.1021/bm900163d](https://doi.org/10.1021/bm900163d)
- Iwamoto S, Nakagaito AN, Yano H (2007) Nano-fibrillation of pulp fibers for the processing of transparent nanocomposites. *Appl Phys A Mater Sci Process* 89:461–466. doi:[10.1007/s00339-007-4175-6](https://doi.org/10.1007/s00339-007-4175-6)
- Iwamoto S, Abe K, Yano H (2008) The effect of hemicelluloses on wood pulp nanofibrillation and nanofiber network characteristics. *Biomacromolecules* 9:1022–1026. doi:[10.1021/bm701157n](https://doi.org/10.1021/bm701157n)
- Iwatake A, Nogi M, Yano H (2008) Cellulose nanofiber-reinforced polylactic acid. *Compos Sci Technol* 68:2103–2106. doi:[10.1016/j.compscitech.2008.03.006](https://doi.org/10.1016/j.compscitech.2008.03.006)
- Johansson A, Aaltonen O, Ylinen P (1987) Organosolv pulping—methods and pulp properties. *Biomass* 13:45–65. doi:[10.1016/0144-4565\(87\)90071-0](https://doi.org/10.1016/0144-4565(87)90071-0)
- Jonoobi M, Harun J, Shakeri A et al (2009) Chemical composition, crystallinity, and thermal degradation of bleached and unbleached kenaf bast (*Hibiscus cannabinus*) pulp and nanofibers. *BioResources* 4:626–639
- Jonoobi M, Khazaeian A, Tahir PM et al (2011) Characteristics of cellulose nanofibers isolated from rubberwood and empty fruit bunches of oil palm using chemo-mechanical process. *Cellulose* 18:1085–1095. doi:[10.1007/s10570-011-9546-7](https://doi.org/10.1007/s10570-011-9546-7)
- Kantouch A, Hebeish A, El-Rafie MH (1970) Action of sodium chlorite on cellulose and cellulose derivatives. *Text Res J* 40:178–184. doi:[10.1177/004051757004000211](https://doi.org/10.1177/004051757004000211)
- Kargarzadeh H, Ahmad I, Abdullah I et al (2012) Effects of hydrolysis conditions on the morphology, crystallinity, and thermal stability of cellulose nanocrystals extracted from kenaf bast fibers. *Cellulose* 19:855–866. doi:[10.1007/s10570-012-9684-6](https://doi.org/10.1007/s10570-012-9684-6)
- Karimi S, Tahir PM, Karimi A et al (2014) Kenaf bast cellulosic fibers hierarchy: a comprehensive approach from micro to nano. *Carbohydr Polym* 101:878–885. doi:[10.1016/j.carbpol.2013.09.106](https://doi.org/10.1016/j.carbpol.2013.09.106)
- Kaushik A, Singh M, Verma G (2010) Green nanocomposites based on thermoplastic starch and steam exploded cellulose nanofibrils from wheat straw. *Carbohydr Polym* 82:337–345. doi:[10.1016/j.carbpol.2010.04.063](https://doi.org/10.1016/j.carbpol.2010.04.063)
- Khristova P, Bentsheva S, Karar I (1998) Soda-AQ pulp blends from kenaf and sunflower stalks. *Bioresour Technol* 66:99–103. doi:[10.1016/S0960-8524\(98\)00058-3](https://doi.org/10.1016/S0960-8524(98)00058-3)
- Knill CJ, Kennedy JF (2003) Degradation of cellulose under alkaline conditions. *Carbohydr Polym* 51:281–300. doi:[10.1016/S0144-8617\(02\)00183-2](https://doi.org/10.1016/S0144-8617(02)00183-2)
- Kose R, Kondo T (2011) Favorable 3D-network formation of chitin nanofibers dispersed in water prepared using aqueous counter collision. *Fiber* 67:91–95. doi:[10.2115/fiber.67.91](https://doi.org/10.2115/fiber.67.91)
- Li J, Henriksson G, Gellerstedt G (2007) Lignin depolymerization/repolymerization and its critical role for delignification of aspen wood by steam explosion. *Bioresour Technol* 98:3061–3068. doi:[10.1016/j.biortech.2006.10.018](https://doi.org/10.1016/j.biortech.2006.10.018)
- Liu A, Walthers A, Ikkala O et al (2011) Clay nanopaper with tough cellulose nanofiber matrix for fire retardancy and gas barrier functions. *Biomacromolecules* 12:633–641. doi:[10.1021/bm101296z](https://doi.org/10.1021/bm101296z)
- Matsuda F, Yamasaki M, Hasunuma T et al (2011) Variation in biomass properties among rice diverse cultivars. *Biosci Biotechnol Biochem* 75:1603–1605. doi:[10.1271/bbb.110082](https://doi.org/10.1271/bbb.110082)
- Mohanty AK, Misra M, Drzal LT (2002) Sustainable biocomposites from renewable resources: opportunities and challenges in the green materials world. *J Polym Environ* 10:19–26. doi:[10.1023/A:1021013921916](https://doi.org/10.1023/A:1021013921916)
- Morimune S, Kotera M, Nishino T et al (2011) Poly(vinyl alcohol) nanocomposites with nanodiamond. *Macromolecules* 44:4415–4421. doi:[10.1021/ma200176r](https://doi.org/10.1021/ma200176r)
- Nagai T, Suzuki N (2000) Isolation of collagen from fish waste material—skin, bone and fins. *Food Chem* 68:277–281. doi:[10.1016/S0308-8146\(99\)00188-0](https://doi.org/10.1016/S0308-8146(99)00188-0)
- Nishino T, Arimoto N (2007) All-cellulose composite prepared by selective dissolving of fiber surface. *Biomacromolecules* 8:2712–2716. doi:[10.1021/bm0703416](https://doi.org/10.1021/bm0703416)
- Nishino T, Takano K, Nakamae K (1995) Elastic modulus of the crystalline regions of cellulose polymorphs. *J Polym Sci, Part B: Polym Phys* 33:1647–1651. doi:[10.1002/polb.1995.090331110](https://doi.org/10.1002/polb.1995.090331110)

- Nishino T, Matsui R, Nakamae K (1999) Elastic modulus of the crystalline regions of chitin and chitosan. *J Polym Sci, Part B: Polym Phys* 37:1191–1196. doi:[10.1002/\(SICI\)1099-0488\(19990601\)37:11<1191::AID-POLB13>3.0.CO;2-H](https://doi.org/10.1002/(SICI)1099-0488(19990601)37:11<1191::AID-POLB13>3.0.CO;2-H)
- Nishino T, Hirao K, Kotera M et al (2003) Kenaf reinforced biodegradable composite. *Compos Sci Technol* 63:1281–1286. doi:[10.1016/S0266-3538\(03\)00099-X](https://doi.org/10.1016/S0266-3538(03)00099-X)
- Nishino T, Matsuda I, Hirao K (2004) All-cellulose composite. *Macromolecules* 37:7683–7687. doi:[10.1021/ma049300h](https://doi.org/10.1021/ma049300h)
- Nogi M, Yano H (2008) Transparent nanocomposites based on cellulose produced by bacteria offer potential innovation in the electronics device industry. *Adv Mater* 20:1849–1852. doi:[10.1002/adma.200702559](https://doi.org/10.1002/adma.200702559)
- Nogi M, Iwamoto S, Nakagaito AN, Yano H (2009) Optically transparent nanofiber paper. *Adv Mater* 21:1595–1598. doi:[10.1002/adma.200803174](https://doi.org/10.1002/adma.200803174)
- Okahisa Y, Yoshida A, Miyaguchi S, Yano H (2009) Optically transparent wood-cellulose nanocomposite as a base substrate for flexible organic light-emitting diode displays. *Compos Sci Technol* 69:1958–1961. doi:[10.1016/j.compscitech.2009.04.017](https://doi.org/10.1016/j.compscitech.2009.04.017)
- Okahisa Y, Abe K, Nogi M et al (2011) Effects of delignification in the production of plant-based cellulose nanofibers for optically transparent nanocomposites. *Compos Sci Technol* 71:1342–1347. doi:[10.1016/j.compscitech.2011.05.006](https://doi.org/10.1016/j.compscitech.2011.05.006)
- Pei A, Butchosa N, Berglund LA, Zhou Q (2013) Surface quaternized cellulose nanofibrils with high water absorbency and adsorption capacity for anionic dyes. *Soft Matter* 9:2047–2055. doi:[10.1039/c2sm27344f](https://doi.org/10.1039/c2sm27344f)
- Petersson L, Kvien I, Oksman K (2007) Structure and thermal properties of poly(lactic acid)/cellulose whiskers nanocomposite materials. *Compos Sci Technol* 67:2535–2544. doi:[10.1016/j.compscitech.2006.12.012](https://doi.org/10.1016/j.compscitech.2006.12.012)
- Puangsin B, Yang Q, Saito T, Isogai A (2013) Comparative characterization of TEMPO-oxidized cellulose nanofibril films prepared from non-wood resources. *Int J Biol Macromol* 59:208–213. doi:[10.1016/j.ijbiomac.2013.04.016](https://doi.org/10.1016/j.ijbiomac.2013.04.016)
- Qua EH, Hornsby PR, Sharma HSS et al (2009) Preparation and characterization of poly(vinyl alcohol) nanocomposites made from cellulose nanofibers. *J Appl Polym Sci* 113:2238–2247. doi:[10.1002/app.30116](https://doi.org/10.1002/app.30116)
- Saito T, Nishiyama Y, Putaux JL et al (2006) Homogeneous suspensions of individualized microfibrils from TEMPO-catalyzed oxidation of native cellulose. *Biomacromolecules* 7:1687–1691. doi:[10.1021/bm060154s](https://doi.org/10.1021/bm060154s)
- Saito T, Kimura S, Nishiyama Y, Isogai A (2007) Cellulose nanofibers prepared by TEMPO-mediated oxidation of native cellulose. *Biomacromolecules* 8:2485–2491. doi:[10.1021/bm0703970](https://doi.org/10.1021/bm0703970)
- Saito T, Kuramae R, Wohlert J et al (2013) An ultrastrong nanofibrillar biomaterial: the strength of single cellulose nanofibrils revealed via sonication-induced fragmentation. *Biomacromolecules* 14:248–253. doi:[10.1021/bm301674e](https://doi.org/10.1021/bm301674e)
- Scheller HV, Ulvskov P (2010) Hemicelluloses. *Annu Rev Plant Biol* 61:263–289. doi:[10.1146/annurev-arplant-042809-112315](https://doi.org/10.1146/annurev-arplant-042809-112315)
- Segal L, Creely JJ, Martin AE, Conrad CM (1959) An empirical method for estimating the degree of crystallinity of native cellulose using the X-ray diffractometer. *Text Res J* 29:786–794. doi:[10.1177/004051755902901003](https://doi.org/10.1177/004051755902901003)
- Soykeabkaew N, Arimoto N, Nishino T, Peijs T (2008) All-cellulose composites by surface selective dissolution of aligned ligno-cellulosic fibres. *Compos Sci Technol* 68:2201–2207. doi:[10.1016/j.compscitech.2008.03.023](https://doi.org/10.1016/j.compscitech.2008.03.023)
- Soykeabkaew N, Nishino T, Peijs T (2009) All-cellulose composites of regenerated cellulose fibres by surface selective dissolution. *Compos Part A Appl Sci Manuf* 40:321–328. doi:[10.1016/j.compositesa.2008.10.021](https://doi.org/10.1016/j.compositesa.2008.10.021)
- Sun RC, Tomkinson J, Ma PL, Liang SF (2000) Comparative study of hemicelluloses from rice straw by alkali and hydrogen peroxide treatments. *Carbohydr Polym* 42:111–122. doi:[10.1016/S0144-8617\(99\)00136-8](https://doi.org/10.1016/S0144-8617(99)00136-8)
- Suzuki K, Okumura H, Kitagawa K et al (2013) Development of continuous process enabling nanofibrillation of pulp and melt compounding. *Cellulose* 20:201–210. doi:[10.1007/s10570-012-9843-9](https://doi.org/10.1007/s10570-012-9843-9)
- Taniguchi T, Okamura K (1998) New films produced from microfibrillated natural fibres. *Polym Int* 47:291–294. doi:[10.1002/\(SICI\)1097-0126\(199811\)47:3<291::AID-PI11>3.0.CO;2-1](https://doi.org/10.1002/(SICI)1097-0126(199811)47:3<291::AID-PI11>3.0.CO;2-1)
- Uetani K, Yano H (2011) Nanofibrillation of wood pulp using a high-speed blender. *Biomacromolecules* 12:348–353. doi:[10.1021/bm101103p](https://doi.org/10.1021/bm101103p)
- Wise LE, Evelyn KR (1947) Quantitative isolation of hemicelluloses and summative analysis of wood. *Inst Pap Chem* 19:459–462. doi:[10.1021/ac60007a010](https://doi.org/10.1021/ac60007a010)
- Wise LE, Maxine M, D'Addieco AA (1946) Chlorite holocellulose, its fractionation and bearing on summative wood analysis and on studies on the hemicelluloses. *Pap Trade J* 122:35–43
- Yang Q, Fujisawa S, Saito T, Isogai A (2012) Improvement of mechanical and oxygen barrier properties of cellulose films by controlling drying conditions of regenerated cellulose hydrogels. *Cellulose* 19:695–703. doi:[10.1007/s10570-012-9683-7](https://doi.org/10.1007/s10570-012-9683-7)
- Yang Q, Saito T, Isogai A (2013) Transparent, flexible, and high-strength regenerated cellulose/saponite nanocomposite films with high gas barrier properties. *J Appl Polym Sci* 130:3168–3174. doi:[10.1002/app.39564](https://doi.org/10.1002/app.39564)
- Yano H, Hirose A, Collins PJ, Yazaki Y (2001) Effects of the removal of matrix substances as a pretreatment in the production of high strength resin impregnated wood based materials. *J Mater Sci Lett* 20:1125–1126. doi:[10.1023/A:1010992307614](https://doi.org/10.1023/A:1010992307614)
- Yousefi H, Nishino T, Faezipour M et al (2011) Direct fabrication of all-cellulose nanocomposite from cellulose microfibrils using ionic liquid-based nanowelding. *Biomacromolecules* 12:4080–4085. doi:[10.1021/bm201147a](https://doi.org/10.1021/bm201147a)
- Zhao HP, Feng XQ, Gao H (2007) Ultrasonic technique for extracting nanofibers from nature materials. *Appl Phys Lett* 90:1–3. doi:[10.1063/1.2450666](https://doi.org/10.1063/1.2450666)